SINGLE PHOTON LIDAR IN MOBILE LASER SCANNING: THE SAMPLING RATE PROBLEM AND INITIAL SOLUTIONS VIA SPATIAL CORRELATIONS

V. V. Lehtola[1,*], H. Hyyti[2], P. Keränen[3], J. Kostamovaara[3]

[1] Department of Earth Observation Science, ITC faculty, University of Twente, Enschede, the Netherlands
[2] Finnish Geospatial Research Institute (FGI), National Land Survey of Finland
[3] Circuits and Systems Research Unit, Faculty of Information Technology and Electrical Engineering, University of Oulu, 90014 Oulu, Finland

Commission II

KEY WORDS: single photon lidar, mobile laser scanning, spatial correlations, detection, ranging, algorithm, outlier, noise

ABSTRACT:

Single photon lidars (in solid state form) offer several benefits over pulsed lidars, such as independence of micro-mechanical moving parts or rotating joints, lower power consumption, faster acquisition rate, and reduced size. When mass produced, they will be cheaper and smaller and thus very attractive for mobile laser scanning applications. However, as these lidars operate by receiving single photons, they are very susceptible to background illumination such as sunlight. In other words, the observations contain a significant amount of noise, or to be specific, outliers. This causes trouble for measurements done in motion, as the sampling rate (i.e. the measurement frequency) should be low and high at the same time. It should be low enough so that target detection is robust, meaning that the targets can be distinguished from the single-photon avalanche diode (SPAD) triggings caused by the background photons. On the other hand, the sampling rate should be high enough to allow for measurements to be done from motion. Quick sampling reduces the probability that a sample gathered during motion would contain data from more than a single target at a specific range. Here, we study the exploitation of spatial correlations that exist between the observations as a mean to overcome this sampling rate paradox. We propose computational methods for short and long range. Our results indicate that the spatial correlations do indeed allow for faster and more robust sampling of measurements, which makes single photon lidars more attractive in (daylight) mobile laser scanning.

1. INTRODUCTION

Mobile laser scanning (MLS) is a less time-consuming and cheaper measurement method than terrestrial laser scanning (TLS) (Puente et al., 2013, Lehtola et al., 2017). The whole idea is based on doing the measurements in motion. Therefore, there is a continuous interest in employing smaller and cheaper measuring equipment that would also consume less and less power. One such device is lidar, and its recent form, single-photon solid-state lidar (Kostamovaara et al., 2015).

Single-photon solid-state lidars, if mass produced, have the potential to become a new standard for autonomous cars, unmanned aerial vehicles, and robotics. In contrast to the traditional pulsed lidars for example, these lidars do not contain any micro-mechanical moving parts (e.g. a rotating mirror) which makes them physically more robust. In addition, the advances in single photon techniques have allowed for a signification reduction in the size of components and power consumption.

However, the nemesis of any single photon lidar is background illumination. Especially, sunlight. Targets illuminated by sunlight pose difficulties for single photon receivers, because the photons from the laser emitter and the photons from the sun are indistinguishable. While mobile mapping may of course be conducted during the night (Vaaja et al., 2018), it would be highly advantageous to be able to operate MLS systems in daylight.

One technique to overcome the problem of indistinguishable photons is to sample multiple of these measurements with respect to time and then try to estimate the range to the target from the obtained distribution. However, methods that require sampling a distribution over time are less useful for MLS, because the sampling becomes difficult, if not impossible, when the sensor is on the move during data acquisition. Hence, it would be imperative to obtain measurements on a high frequency so that they can be relied upon.

Outlier-free ranging data is especially needed for simultaneous localization and mapping (SLAM), which is behind all the above mentioned applications. SLAM technique uses the ranging data to construct a map of the environment, and then utilizes overlaps in the data to update the position of the moving platform on that map (Bailey, Durrant-Whyte, 2006, Nüchter et al., 2007, Kohlbrecher et al., 2011, Cadena et al., 2016, Karam et al., 2019). The map building and position updating are conducted simultaneously and as processes are very susceptible to outliers in the ranging data. For these reasons, the filtering of abundant outliers before SLAM (i.e. registration) has been studied in (Lehtola et al., 2016b, Lehtola et al., 2016a), and in more general form addressing spatial correlations in (Lehtola et al., 2019). However, these works do not utilize a single photon lidar. And from a study conducted for airborne lidars, it is known that single photon and full-wave form lidars have different measurement properties (Mandlburger et al., 2019). Hence, the question whether these lidars would be useful in MLS boils down to whether the outliers from background illumination be filtered out of the single photon data.

Therefore, in this paper, we focus on examining the data obtained from a 256 channel single-photon solid-state lidar (Keränen, Kostamovaara, 2018). Our purpose is to adapt and utilize the

*Corresponding author: ville.lehtola@iki.fi

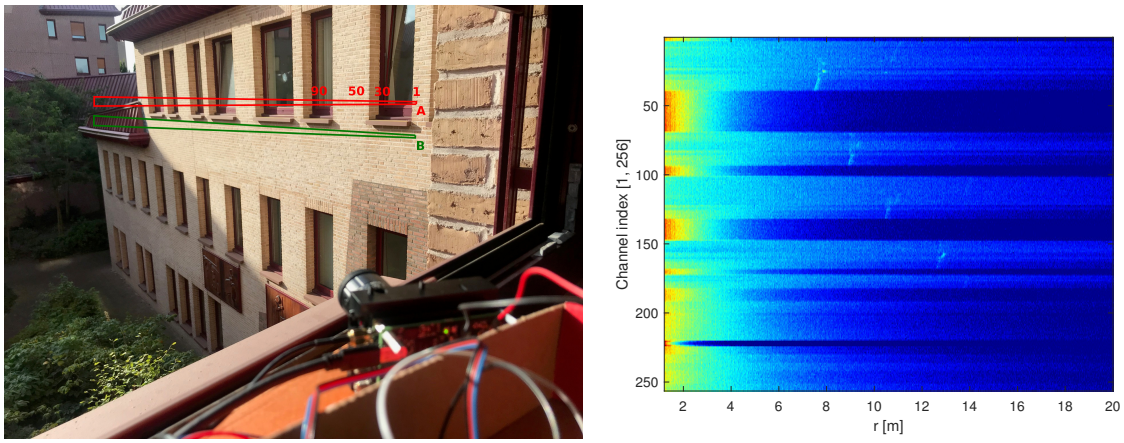

Figure 1. (a) Outdoor measurement setup. The laser stripe (approx. 0.3°x 37°) covers bright and darker areas of the wall. Its approximate shapes for two separate measurements are drawn with a red line (measurement A during sunlight) and with green line (measurement B during overcast). (b) Detection of sunlight illuminated targets is impossible (measurement A), because SPADs are flooded with background illumination photons, which trigger early detection immediately when the SPADs are ready for reception (shown with red color, e.g. near channel 50). Shaded surfaces are also almost undetectable (e.g. see the cyan patterns near channels 30 and 90, at 8 to 12 m range).

techniques for outlier filtering before data registration from (Lehtola et al., 2019). We shall study data captured during daylight and from targets illuminated by direct sunlight. The algorithm we propose is computationally simple, so that it could be embedded on chip and run online. This is necessary because, for example, the single photon lidar studied here outputs some 36 million observations per second.

For lidar measurements, the time of flight is linearly proportional to the ranging distance. Therefore, spatial correlations can have an ambiguous meaning. By spatial correlations, here, we mean that if we correlate observations, all non-noise correlations are caused by the spatial environment of the lidar. This helps us to distinguish 'signal' from the noise, because the background photons are not correlated and the back-scattered photons are. Importantly, our method is self-sufficient, i.e., it does not require any additional sensors or external data.

The paper is organized as follows. The related work is reviewed in Section 2, including those works on the hardware of the single photon lidar. In Section 3, we propose two algorithms, one for the short range and one for the long range. Section 4 introduces data capturing conditions. Results are in Section 5 and Section 6 concludes the paper.

2. RELATED WORK

A single-photon solid-state lidar consist of a laser emitter, from which the beam is sprayed or split using static optics, and a receiver grid, which can observe the back-scattered photons from a wide angle (Kostamovaara et al., 2015). The receiver grid is a single-photon avalance diode (SPAD) array. Recent advances in SPAD technology have yielded high pixel count imagers which enable fast acquisition rates and sensitivity to individual photons (Gyongy et al., 2018). Since there are multiple small-size receivers close to one another, measures have been taken to reduce the crosstalk between the neighboring receivers (Jahromi, Kostamovaara, 2018).

The experimental single-photon solid-state lidar that we use here is presented in and has been assembled by the authors of (Keränen, Kostamovaara, 2019), see Figure 1 (a). It is an advanced design of the one in (Keränen, Kostamovaara, 2018). The lidar has a range of up to 96 m (640 ns) and an opening angle of about 37 degrees. It has a set of optics to eliminate background illumination in front of the receiver array, including a 810 nm single-band bandpass filter. Also, the angle of incidence must be close to be one meant for the photons coming from the emitter. The scanner is essentially a line scanner. However, in contrast to (Keränen, Kostamovaara, 2018), each channel has 8 receivers, i.e. single photon avalanche diodes (SPADs), stacked on top of one another (Keränen, Kostamovaara, 2019). The digital to time converter (TDC) outputs the signal from the SPAD that triggers first. The laser has a 140 kHz emission frequency, and the observations from the same pulse are time-synchronized with respect to this. Additionally, a pulse-per-second (PPS) time synchronization option is provided for multi-sensor integration purposes.

Every single photon detection, i.e. SPAD trigging, is followed by a dead time, during which the SPAD is recharging and photons that pile up on the detector are not detected. Therefore, the observed photon distribution differs from the original photon arrival distribution. This original photon arrival distribution is typically Poissonian, and can be estimated from the observations as a post-processing step (Pediredla et al., 2018). Here, however, we seek to shortcut the (histogram) sampling phase by relying in spatial correlations (Lehtola et al., 2019). This hopefully leads onto a more computationally efficient methodology that could be used to pre-process the data on-chip (e.g. the 36M range observations per second that we obtain).

Single photon lidars have been used in airborne laser scanning (ALS) to see whether they can replace traditional (full-waveform or pulsed) lidars (Mandlburger et al., 2019, Degnan, 2016). The measurement geometry for a single photon lidar from an aeroplane is more favourable than in MLS, as a priori about the range to the target can be formed. In MLS, the targets can lie anywhere within the detection range[1], starting from one meter to the maximum range, while in ALS, if the fly altitude is 1000 meters and the targets are 100 meters high, they are detected within 10% of the detectable range. This is important because

[1] In MLS, the orientation of the platform can change rapidly, causing the viewed scene to change.

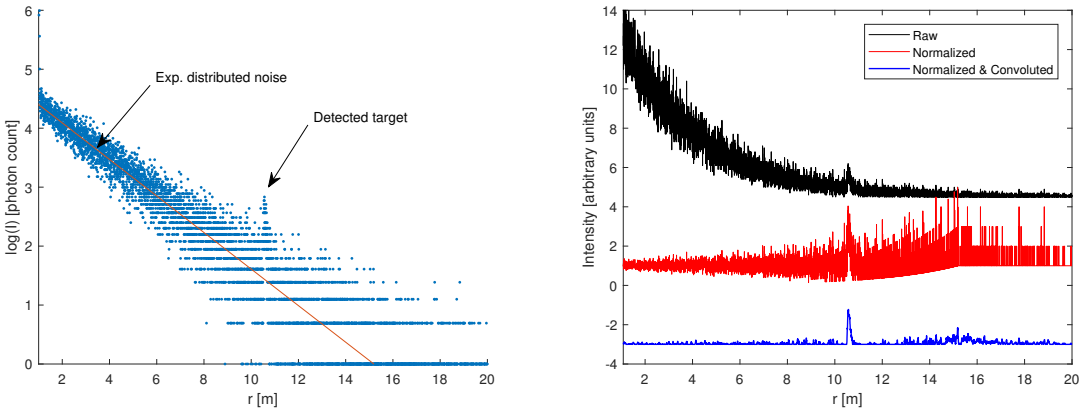

Figure 2. Traditional signal processing for range detection. (a) Exponential noise distribution f_N is visible from a channel detecting a target not illuminated by direct sunlight. The target can be detected only after sampling (and processing) the signal (here: the sample size is 100 000). The line is from an exponential function and it is drawn to guide the eye. (b) Processing of the raw signal by normalizing with respect to the exponential noise distribution f_N and by convolution (here: 3.81 cm wide uniform kernel). The estimated (red) signal peak area to the total (black) area is 0.18%.

the background illumination declines exponentially as a function of the range, when only one photon detection per emitted pulse per channel (or pixel) is recorded, as in (Keränen, Kostamovaara, 2019). Hence, such single photon detection benefits from a priori knowledge about the detection range in normalizing this exponential distribution away.

3. METHOD

All photons of equal wavelength (here 810 nm) are indistinguishable from each other. Hence, the photons back-scattered from a detectable object are indistinguishable from the ones from background illumination. In other words, we cannot say whether any single SPAD trigging was caused by signal or noise, and therefore any single trigging is meaningless per se. Therefore, observations must be either correlated or sampled. For short range ($\sim$ 2 m), we propose a straightforward correlation approach. For long range ($\sim$ 10 m and above), observations are dominated by background illumination that forms an exponentially decaying shape with respect to the detected range. See Figure 2 on traditional signal processing with respect to this exponential distribution. Hence, we shall adapt the spatial correlation scheme with the traditional signal processing approach.

3.1 Short range detection

We study whether the use of spatial correlations can help to distinguish background illumination from the true signal. For this, we adapt the methodology presented in (Lehtola et al., 2019) and previously in (Lehtola et al., 2016b) as follows. The single-photon solid-state lidar observations consist of range measurements from single photons

$$r_{i_n} \equiv r(i_n), \tag{1}$$

where r_{i_n} is the measured range, i_n is the (chronological) index number of the scan point recorded in channel $n \in [1, M]$. Here, the length of each scan line is $M = 256$ channels (Keränen, Kostamovaara, 2019).

We define that a measurement r_{i_n} of Eq. (1) is supported by spatial correlations, $r_{i_n} \in S_b$, if the cover of supporting measurements C in its neighborhood $N(i_n)$ satisfies $C \geq \rho_c \, |N(i_n)|$, where we choose $\rho_c = 1/2$ to define a minimum support cover density. Formally,

$$r_{i_n} \in S_b \quad \text{if} \quad C_{i_n} \geq \rho_c \, |N(i_n)|, \tag{2}$$

where

$$C_{i_n} = \sum_{j \in N(i_n)} \delta_{ij} \,, \quad \delta_{ij} = \begin{cases} 1, & if \; |r_{i_n} - r_{j_n}| < \xi \\ 0, & otherwise \end{cases} \,, \tag{3}$$

with the support threshold[2] $\xi = 8.8$ cm (3 ns) and

$$N(i_n) \equiv \{r_{i_n-1}, r_{i_n+1}\} \tag{4}$$

In words, the neighborhood $N(i_n)$ of Eq. (4) includes the chronologically previous and the next measurement observed in the same channel n. While doing computations, only three consecutive measurements in each channel is required to be kept in memory. That is, a total of $3 \times M$ observations. Eq. (4) is the simplest form of the spatial correlation neighborhoods and can yield output with a very high frequency, which is advantageous for MLS applications.

3.2 Long range detection

All the SPAD gates are opened simultaneously for measurement (Keränen, Kostamovaara, 2019) and for a constant light flux of background illumination, for each SPAD, there is a constant probability per time unit that a background photon triggers that SPAD. Specifically, background photon arrivals are Poisson distributed. In long range detection, the gate is open for a longer time and thus the probability of observing noise is higher than at short range. Moreover, at long range, the probability of a back-scattered 'signal' photon trigging a SPAD is lower than at short range, since the back-scattered photon flux weakens with respect to range. This leads into an unwanted side effect that the observed arrival distribution contains an exponential noise tail also beyond the detected target. In other words, if the pulse photons are back-scattered elsewhere than on the SPAD, the SPAD remains open for detection and can trigger on a background photon.

[2] See (Lehtola et al., 2019) for an elaborate discussion on the support threshold parameter and what it manifests.

The support technique can deal with noise but it has its limits. In (Lehtola et al., 2019), limited target detection (tree trunk points) is plausible even when these measurements consist of 5% of the total data. Here, as shown in Figure 2, the observations from the target get drowned in the noise as they consist only of about 0.18 % of the data (ratio between the area of red exp-normalized peak and the area of the black curve). Hence, the signal needs de-noising of over one degree of magnitude. Another reason to de-noise the signal is that the exponential distribution of the noise otherwise introduces a correlation pattern in the noise and that this numerical correlation is indistinguishable from spatial correlations within the support scheme. Therefore, in order to utilize spatial correlations in long range detection, observations must be normalized against the exponential noise distribution.

For normalization, the observations need to be sampled. The experimental noise distribution is ideally sampled from the observed data itself, and not from external sources, since SPAD instrumentation noise is present in addition to the triggings made by background photons. Furthermore, because the amount of background illumination may change during a measurement done in motion as scene lighting changes, the noise distribution should be adaptive in that it is sampled simultaneously as range detection is performed. Hence, we model the noise distribution directly from the sample, such as the one in Figure 2 (a), and pre-process the signal as in Figure 2 (b) but with a smaller sample size as explained in the following. These steps are done as in the baseline method used in (Keränen, Kostamovaara, 2019, Keränen, Kostamovaara, 2018).

When measuring from motion, the trade-off in histogramming (i.e. sampling) the distribution is one between the range resolution and the sampling time. For example, keeping a range resolution of 3 mm in the 96 m range results in 32000 bins which in turn set a numerical lower limit for the sampling time (i.e. sample size). A following adequate rate of around 20 Hz is less than what in authors' expertise would be preferred for MLS measurements ($\geq$ 100 Hz). Therefore, we attempt to perform fast sampling in conjunction with the support scheme in order to obtain an output with high frequency and adequate reliability.

The sample size is set to 1400, so that the operational measuring frequency is the sought after 100 Hz. Each sample is then normalized and convoluted, as in Figure 2 (b). The proposed support scheme is then utilized to filter out unsupported peak positions. To this end, a suitable support mask is chosen. Here, we use a cross-channel neighborhood, namely

$$N_{\text{longrange,cross}}(i_n) \equiv \{r_{i_{n-2}}, r_{i_{n-1}}, r_{i_{n+1}}, r_{i_{n+2}}\} \quad (5)$$

and select the range-wise first supported observation for each channel, $C \geq 1$. As the observations are not points but intensity distributions, the range condition in Eq. (3) is modified into the form

$$|\rho(i_n, r_k)\rho(j_m, r_k)| > \xi_\rho, \quad (6)$$

where i_n and j_m are the two trial observations (i.e. distributions), r_k marks the midpoint of the histogram bin and is looped over, and ξ_ρ is a constant intensity threshold that follows from the normalization. In other words, the adjacent channel observations are used for support so that the probability to detect the backscattering peaks increases. Finally, the position of the range-wise first supported peak is obtained for each channel, resulting in a single range observation for each channel and for each pulse emission time, i.e. r_{i_n} of Eq. (1).

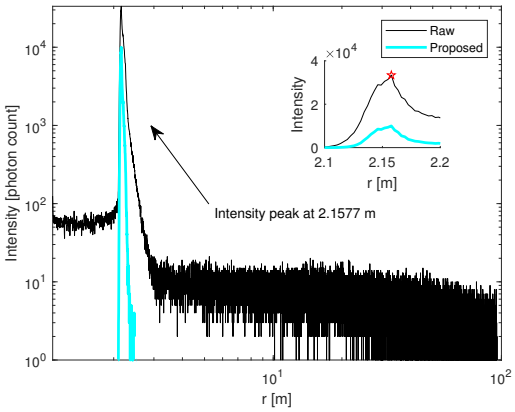

Figure 3. Short range detection results. Distribution of range observations r_{i_n} from one channel, $n = 127$, when sampling over time in nominal conditions. Raw data from the single photon lidar (black) is filtered from outliers using the proposed technique (cyan). Target, i.e. an indoor wall, is detected near 2.1577 meters. The inset figure shows that the peak location is unchanged by the proposed technique.

In order to get rid of the numerical correlations that follow from low data population at the distribution tails (see the Results section), another support check is made for each channel using consecutive observations

$$N_{\text{longrange,line}}(i_n) \equiv \{r_{i_n-1}, r_{i_n+1}\}, \quad (7)$$

similar to the short range case, with $\xi = 0.05$ m. Then the supported ranges, $r_{i_n} \in S_b$, are converted into xy-coordinates in the sensor frame.

The physical size of the support kernel in Eq. (5) for spatial correlations is comparable to the size of the convolution kernel, $w = 3.81$ cm, used in the baseline method for signal processing, see Figure 2 (b). At a 14 m range, beams into two adjacent channels of our lidar are 3.8 cm apart. Hence, using observations from adjacent channels and observations within $\pm w/2$ length for support can be seen as reasonable.

4. DATA AND EQUIPMENT

Data is captured in two setups that we call short range (indoor, no image) and long range (outdoor, see Figure 1 (a)). The lidar data is obtained through an USB-C connection. Short range measurements are up to 3 meters and contain less background noise as they are performed in indoor conditions during the day. Long range measurements are up to 14 meters and contain more noise in form of background illumination due to sunlight. Surfaces illuminated by sunlight (measurement A) are not detectable in time frames intended for mobile scanning, as can be seen from Figure 1 (b). For long range detection, we therefore capture data also during overcast when the wall surface is not illuminated by direct sunlight (measurement B).

In the Results section, we analyze (i) the short range data and (ii) the long range data captured during overcast (measurement B).

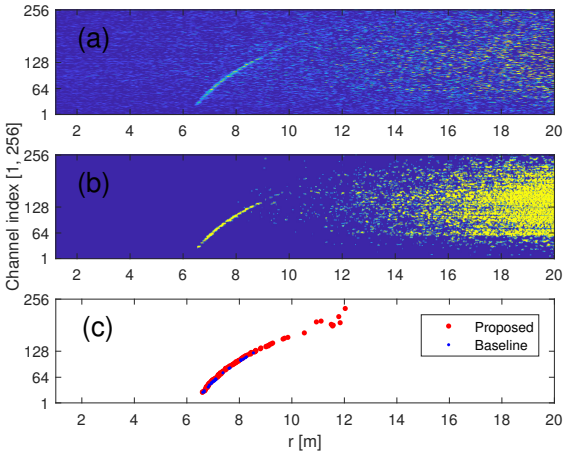

Figure 4. Long range detection, visualization of one measurement sample from each channel with (a) baseline and (b) the proposed method. (c) Supported ranges, $r_{i_n} \in S_b$, versus the baseline ranges. The target is a straight brick wall shown in a green box in Figure 1, measurement B data.

Measurement B is taken from the approximate location marked with green lines in Figure 1 (a).

5. RESULTS

The proposed short range algorithm (Section 3.1) reduces outliers but also results in a loss of measurements in total, see the sharpened and lowered distribution in Figure 3. The highest peak location of the distribution is retained as can be seen from the figure inset. Hence, single measurements filtered with the proposed method do very probably indicate the range to the target. This may form a major step forward in on-the-fly processing of the gargantuan amount of data that the lidar outputs (500 Mb/s). Bypassing the sampling scheme that the proposed method does may come at an expense in range precision. Judging from the width of the second peak this would lead into a ranging error with a standard deviation of $\sigma = 3$ cm and a maximum error of ± 20 cm for supported individual measurements at a range of 2.15 m.

Figure 4 visualizes the long range detection for the baseline (Keränen, Kostamovaara, 2019, Keränen, Kostamovaara, 2018) and the spatial correlation methodology for one sample recorded with the fast sampling rate of 100 Hz. The problem when using the baseline method, see (a), is that range determination is hard and uncertain because of the small sample size and the abundance of background noise. On the other hand, when correlating observations from adjacent channels, see (b), most of the background noise is eliminated. In this mid-term result, the sample tails appear to be strongly correlated between the SPAD channels. These correlations at the distribution tails are caused by numerical effects, i.e. by that that the amount of data is small, and vanish when we self-correlate these observations with respect to time. The channel self-correlation is done similarly as in the short range case, see Eqs. (3) and (4). Afterwards, the xy-coordinates for the points are calculated in the sensor frame using the sensor design properties.

Finally, we test the repeatability of detection. As in all tests of this paper, the test setup is static, and the same detection should be acquired from each laser pulse. However, as the sample size

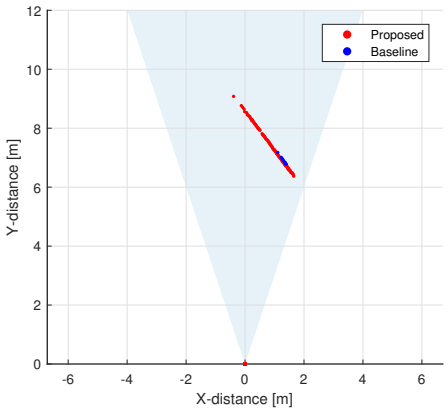

Figure 5. Long range detection, xy-plot with the baseline (blue) and the proposed method (green). The target is a straight brick wall shown in a green box in Figure 1. Only the observations that have at least 50% repeatability are shown. This is the follow-up result from Figure 4 for range determination.

is limited to 1400 laser pulses, all detection is uncertain because of the background illumination. We compare the baseline method against the proposed method. Results are shown in xy-coordinates that are in the sensor frame, see Figure 5. Only the observations that have at least 50% repeatability are shown. We conclude that the use of spatial correlations increases the robustness of detection and ranging.

6. DISCUSSION

The strengths and weaknesses of single photon lidar technology for MLS are evaluated in Table 1. Currently, the limiting factor is the vulnerability to background illumination which leads to elongated sampling times. We address this issue by proposing a method that extends the range of operational conditions where the single photon techniques can be used by allowing for the shortening of sampling times in daylight conditions. This does right to the hardware, which works well in low ambient light conditions. For example with a static measurement geometry and the baseline method, the used experimental single photon lidar can measure distances up to 30 meters at 28fps with an accuracy and precision of $\pm$2mm and $<$ 1cm, respectively (Keränen, Kostamovaara, 2019). In theory, the background illumination problem might also be remedied from the hardware side if very large pulse energies could be created in the in the short pulse mode, $<$ 1 ns, which would allow for accurate timing with large waves of photons (Kostamovaara et al., 2015).

In order to counter the effects of background illumination, the objectives for developing computational single photon methodology for mobile laser scanning are to

- increase the sampling rate so that measurements can be done from motion,
- assess and increase the reliability of measurements,
- perform these tasks in a self-calibration manner (i.e. without external radiometric sensors), and
- perform these tasks automatically and online, i.e. while measuring from motion.

Property	Preferable for MLS	Traditional lidar	Single photon lidar
Line measurement rate	≥100 Hz	10–100 Hz	28–50 Hz (baseline) 100 Hz (proposed method)
Daylight operations	Yes	Yes	Limited
Nighttime operations	Yes	Yes	Yes
Mechanical robustness	High	Low	High
Equipment size	Small	Large	Small
Power consumption	Small	Large	Small

Table 1. Strengths and weaknesses of single photon lidar in mobile laser scanning. Preferences follow from authors' expertise.

As a nice example external to our work, (Pediredla et al., 2018) show how to compensate for the photon pile-up effect in post-processing computation without external data. Note that, ideally, as the data stream can consist of dozens of observations per second, the algorithms working on the stream of data are simple and fast and run with a limited cache size.

The lidar used here captures photons in a vertical 0.3 degree angle using 8 SPADs stacked on top of one another in one channel. This design is ideal for a dual-purpose: short and long range. In a few meters distance, the probability that a back-scattered photon triggers one of these 8 SPADs is high, which results into a measurement from that channel. However, as distance to the target increases, the return angle of the back-scattered photons decreases, leading to that some SPAD orientations become unreachable. As a consequence, these unreachable SPADs contribute only triggings from background illumination, i.e. noise. Therefore, in order to retain a sufficient signal to noise ratio in long range, the SPADs at the side of the array can be turned off. At the moment, this must be done manually. Therefore, there is a need for an autonomous control loop to adjust the opening and closing of the SPADs, if benefits from long range (up to 96 m) and close range detection of the SPAD array design are simultaneously to be reaped. This is a subject for future work.

Another subject for future work would be adaptive gating. If there would be means to have a rough a-priori estimate for the range before the measurement, then the measurement could be obtained with a tighter gating. That is, the gate could be opened just before the back-scattering is expected and then closed afterwards. In principle, an adaptive gating scheme for SPADs would allow for more robust detection at short and at long range – and also when measuring from motion.

7. CONCLUSION

Spatial correlations are demonstrated to be usable at different ranges and noise levels, although significant pre- and post-processing are necessary if a signal is really noisy. With the term spatial correlations, we refer to all correlations that are not noise, because these are caused by the spatial environment of the lidar. Most part of the noise in the data is due to background illumination caused by sunlight.

At short range and in indoor conditions, it is plausible to directly exploit the correlations between individual observations. These correlations are spatial because the back-scattered photons are from the same physical target. This allows for short-cutting algorithm-wise, as signal sampling is not necessary in this case.

At our long range setup, the relative amount of (Poissonian) noise consists more than 99% of observations even though the target surface is not illuminated by direct sunlight. Due to the abundant noise, using the traditional steps of signal sampling, normalization of the exponential noise distribution, and signal convolution are necessary as pre-processing operations. After this pre-processing, we propose the use of spatial correlations by adapting the support scheme from (Lehtola et al., 2019). The support scheme is modified to evaluate pairs of sample distributions, i.e. cross-channel correlations. These correlations eliminate random noise but cannot deal with numerically correlated noisy tails, which in turn can be dealt by using self-correlations over single channels.

We conclude that the proposed self-sufficient computational method for long range extends the range of operational conditions where single photon techniques can be used, especially, in daylight. Furthermore, we expect that the signal processing steps proposed here would allow for an adequate increase in the sampling rate (up to e.g. 100 Hz) so that single photon lidars could be employed more widely in mobile laser scanning (MLS). Finally, we note that the development of single photon lidars is heading toward 3D scanners, meaning lidars that have a 2D SPAD grid. These lidars will also very likely benefit from the proposed methodology.

8. ACKNOWLEDGMENTS

Academy of Finland is acknowledged for financial support for project 'Centre of Excellence in Laser Scanning Research' (CoE-LaSR) (272195). Strategic Research Council at the Academy of Finland is acknowledged for financial support for project 'Competence Based Growth Through Integrated Disruptive Technologies of 3D Digitalization, Robotics, Geospatial Information and Image Processing/Computing - Point Cloud Ecosystem (293389 / 314312)'.

REFERENCES

Bailey, T., Durrant-Whyte, H., 2006. Simultaneous localization and mapping (SLAM): Part II. *IEEE Robotics & Automation Magazine*, 13(3), 108–117.

Cadena, C., Carlone, L., Carrillo, H., Latif, Y., Scaramuzza, D., Neira, J., Reid, I., Leonard, J. J., 2016. Past, present, and future of simultaneous localization and mapping: Toward the robust-perception age. *IEEE Transactions on robotics*, 32(6), 1309–1332.

Degnan, J., 2016. Scanning, multibeam, single photon lidars for rapid, large scale, high resolution, topographic and bathymetric mapping. *Remote Sensing*, 8(11), 958.

Gyongy, I., Al Abbas, T., Finlayson, N., Johnston, N., Calder, N., Erdogan, A., Dutton, N. W., Walker, R., Henderson, R. K., 2018. Advances in cmos spad sensors for lidar applications. *Emerging Imaging and Sensing Technologies for Security and Defence III; and Unmanned Sensors, Systems, and Countermeasures*, 10799, International Society for Optics and Photonics, 1079907.

Jahromi, S., Kostamovaara, J., 2018. Timing and probability of crosstalk in a dense CMOS SPAD array in pulsed TOF applications. *Optics express*, 26(16), 20622–20632.

Karam, S., Vosselman, G., Peter, M., Hosseinyalamdary, S., Lehtola, V., 2019. Design, Calibration, and Evaluation of a Backpack Indoor Mobile Mapping System. *Remote sensing*, 11(8), 905.

Keränen, P., Kostamovaara, J., 2018. 256 x TDC Array With Cyclic Interpolators Based on Calibration-Free 2x Time Amplifier. *IEEE Transactions on Circuits and Systems I: Regular Papers*, PP, 1-10.

Keränen, P., Kostamovaara, J., 2019. 256x8 SPAD Array With 256 Column TDCs for a Line Profiling Laser Radar. *IEEE Transactions on Circuits and Systems I: Regular Papers*, PP, 1-12.

Kohlbrecher, S., Meyer, J., von Stryk, O., Klingauf, U., 2011. A flexible and scalable slam system with full 3d motion estimation. *Proc. IEEE International Symposium on Safety, Security and Rescue Robotics (SSRR)*, IEEE.

Kostamovaara, J., Huikari, J., Hallman, L., Nissinen, I., Nissinen, J., Rapakko, H., Avrutin, E., Ryvkin, B., 2015. On laser ranging based on high-speed/energy laser diode pulses and single-photon detection techniques. *IEEE Photonics Journal*, 7(2), 1–15.

Lehtola, V., Kaartinen, H., Nüchter, A., Kaijaluoto, R., Kukko, A., Litkey, P., Honkavaara, E., Rosnell, T., Vaaja, M., Virtanen, J.-P. et al., 2017. Comparison of the selected state-of-the-art 3D indoor scanning and point cloud generation methods. *Remote sensing*, 9(8), 796.

Lehtola, V. V., Lehtomäki, M., Hyyti, H., Kaijaluoto, R., Kukko, A., Kaartinen, H., Hyyppä, J., 2019. Preregistration Classification of Mobile LIDAR Data Using Spatial Correlations. *IEEE Transactions on Geoscience and Remote Sensing*.

Lehtola, V. V., Virtanen, J.-P., Vaaja, M. T., Hyyppä, H., Nüchter, A., 2016a. Localization of a mobile laser scanner via dimensional reduction. *ISPRS journal of photogrammetry and remote sensing*, 121, 48–59.

Lehtola, V., Virtanen, J.-P., Rönnholm, P., Nüchter, A., 2016b. Localization corrections for mobile laser scanner using local support-based outlier filtering. *ISPRS Annals of the Photogrammetry, Remote Sensing and Spatial Information Sciences*, 3, 81.

Mandlburger, G., Lehner, H., Pfeifer, N., 2019. a Comparison of Single Photon and Full Waveform LIDAR. *ISPRS Annals of Photogrammetry, Remote Sensing and Spatial Information Sciences*, 397–404.

Nüchter, A., Lingemann, K., Hertzberg, J., Surmann, H., 2007. 6D SLAM3D mapping outdoor environments. *Journal of Field Robotics*, 24(8-9), 699–722.

Pediredla, A. K., Sankaranarayanan, A. C., Buttafava, M., Tosi, A., Veeraraghavan, A., 2018. Signal processing based pile-up compensation for gated single-photon avalanche diodes. *arXiv preprint arXiv:1806.07437*.

Puente, I., González-Jorge, H., Martínez-Sánchez, J., Arias, P., 2013. Review of mobile mapping and surveying technologies. *Measurement*, 46(7), 2127–2145.

Vaaja, M., Kurkela, M., Maksimainen, M., Virtanen, J.-P., Kukko, A., Lehtola, V. V., Hyyppä, J., Hyyppä, H. et al., 2018. Mobile mapping of night-time road environment lighting conditions. *Photogrammetric journal of Finland*, 26(1).